

Optimum Noise Mechanism for Differentially Private Queries in Discrete Finite Sets

Sachin Kadam, Anna Scaglione, Nikhil Ravi, Sean Peisert, Brent Lunghino, and Aram Shumavon

Abstract—Most published work on differential privacy (DP) focuses exclusively on meeting privacy constraints, by adding to the query noise with a pre-specified parametric distribution model, typically with one or two degrees of freedom. The accuracy of the response and its utility to the intended use are frequently overlooked. Considering that several database queries are categorical in nature (e.g., a label, a ranking, etc.), or can be quantized, the parameters that define the randomized mechanism’s distribution are finite. Thus, it is reasonable to search through numerical optimization for the probability masses that meet the privacy constraints while minimizing the query distortion. Considering the modulo summation of random noise as the DP mechanism, the goal of this paper is to introduce a tractable framework to design the optimum noise probability mass function (PMF) for database queries with a discrete and finite set, optimizing with an expected distortion metric for a given (ϵ, δ) . We first show that the optimum PMF can be obtained by solving a mixed integer linear program (MILP). Then, we derive closed-form solutions for the optimum PMF that minimize the probability of error for two special cases. We show numerically that the proposed optimal mechanisms significantly outperform the state-of-the-art.

Index Terms—Differential Privacy, Optimum Noise Mechanism, Discrete Queries, MILP, Optimal Error Rate

1 INTRODUCTION

DIFFERENTIAL PRIVACY (DP) is a technique used for publishing database queries concealing confidential attributes. Some of its real-world applications are in the publication of: the US Census 2020 data (using disclosure avoidance system (DAS) [1]), Google’s historical traffic statistics [2], Microsoft’s telemetry data [3], LinkedIn user engagement information to third parties for advertisements [4], etc. DP hinges on a randomized mechanism through which the data publisher, who owns the database, responds to the queries of an analyst so that queries to data that differ by a specific attribute generate a similar distribution of query answers, which in turn makes it statistically hard to reveal whether or not data with that specific attribute were embedded in the query computations.

To randomize the query answers, most published literature relies on adding noise to the query result, with a parametric distribution featuring one or two degrees of freedom. In this paper, we propose to optimize all the parameters of the probability mass function (PMF) for a categorical query with finite discrete answers so that the randomized query outcome meets the DP constraints while minimizing the expected distortion for a certain database and discrete finite set of answers.

Prior to outlining our contributions, next, we review the relevant literature.

1.1 Literature review

In literature, several papers studied the additive noise mechanisms for discrete query outputs [5], [6], [7]. For discrete queries with infinite support, the additive noise mechanism for ϵ -differential privacy that minimizes any convex function of the query error was found in [5]; the optimum PMF is shown to have a specific decreasing staircase trend. The problem of finding the optimal data-independent noise mechanism for ϵ -differential privacy is addressed also in [6]. Even though the authors focus on continuous query outputs, they claim one can extend easily the method to discrete queries. Neither paper [5], [6] explored the optimization of the (ϵ, δ) -differential privacy trade-off for $\delta > 0$. For integer query outputs the optimal noise mechanism design for (ϵ, δ) -differential privacy is the subject of [7]. Another approach to integer count query is carried out in [8], where a double-sided geometric distribution noise mechanism is used. A recent study on the count query DP problem is found in [9], in which the authors use a set of constrained mechanisms that achieve favorable DP properties. The related problem of publishing the number of users with sensitive attributes from a database is addressed in [10]. In their proposed DP mechanism, they add an integer-valued noise before publishing it to protect the privacy of individuals. Though the randomized query response, produced by the proposed mechanism in [10], lies in the actual query support range, the additive noise PMF used depends on the query output, which requires storing several PMFs. In the context of discrete queries, an additive discrete Gaussian noise-based mechanism is proposed in [11]. They show that the addition of discrete Gaussian noise provides the same privacy and accuracy guarantees as the addition of continuous Gaussian noise.

- S. Kadam is with Sungkyunkwan University, e-mail: sachinkadam@skku.edu.
- A. Scaglione and N. Ravi are with Cornell Tech., e-mail: {as337,nr337}@cornell.edu.
- S. Peisert is with Lawrence Berkeley National Laboratory, e-mail: speisert@lbl.gov.
- B. Lunghino and A. Shumavon are with Kevala, Inc., e-mail: {brent, aram}@kevalaanalytics.com.

This research was supported by the Director, Cybersecurity, Energy Security, and Emergency Response, Cybersecurity for Energy Delivery Systems program, of the U.S. Department of Energy, under contract DE-AC02-05CH11231. Any opinions, findings, conclusions, or recommendations expressed in this material are those of the authors and do not necessarily reflect those of the sponsors of this work.

1.2 Paper contributions

This paper revisits the design of DP random mechanisms to ensure query answers are (ϵ, δ) -differentially private, for queries that can have $n + 1$ possible answers, each mapped onto one of the numbers between $0, \dots, n$. The mechanism we study is the modulo $n + 1$ addition of noise.

In Section 3.1 we show that, for a given (ϵ, δ) budget, the additive noise PMF that minimizes a linear error metric can be obtained as the solution of a MILP in general. Note that, for the case $\delta = 0$ it is already known that optimum PMF can be found as the solution of an LP problem [12], which is a special case of our general formulation. We then derive the explicit expression of the optimum PMF giving a minimum error for a certain (ϵ, δ) pair for two special cases in Sections 3.2.1 and 3.2.2 (which subsumes the result in [12]). The two cases define specific ways in which data X and X' , that differ because of a sensitive attribute change, can affect the modulo n differences of the query answers. In both cases, we derive the parameters of the error rate function $\rho(\epsilon, \delta)$ showing that it is piece-wise linear. The structure of the optimum PMF and error rate allows us to specify that the optimum (ϵ, δ) trade-off curve for a given error rate is decreasing exponentially as δ increases with a discrete set of discontinuities that prelude a change in the exponential rate of decay as ϵ increases. All of these results are corroborated by our numerical analysis in Section 4 through comparisons of our method with the prior art.

1.3 Notation

Let $\mathbb{N}, \mathbb{N}^+, \mathbb{Z}, \mathbb{R}$ denote the sets of natural numbers including zero, natural numbers excluding zero, integers, and real numbers, respectively. The set integers $\{0, 1, \dots, n\}$, $n \in \mathbb{N}$, is referred to as $[n]$, $[n]_+$ is, instead, $\{1, \dots, n\}$. $\lfloor k \rfloor$ and $\lceil k \rceil$ denote the floor and ceiling function of k , respectively. $|\mathcal{A}|$ denotes the cardinality of set \mathcal{A} , and $\mathcal{A} \setminus \mathcal{B}$ denotes the set difference. $\mathbb{Q}(X)$ refers to the query function applied on the data X from a database, denoted by \mathcal{X} . \mathcal{Q} denotes a discrete finite set of query answers. In this paper, the query domain is discrete and finite and mapped onto the set $[n]$ of size $n + 1$. The numerical outcome of the query will be denoted by the variable $q \in [n]$ while \tilde{q} will denote the outcome after the randomized publication, with distribution $f(\tilde{q}|X)$. For vector queries, whose outcome \mathbf{q} is within a finite discrete domain one can always map the result onto the set $[n]$, hence the optimization we propose applies. We omit the suffix η from the noise distribution $f_\eta(\eta)$ using the notation $f(\eta)$ whenever possible without causing confusion.

2 PRELIMINARIES

Definition 1 ((ϵ, δ) -Differential Privacy (DP) [13]). *A randomized mechanism $\tilde{q} : \mathcal{Q} \rightarrow \mathcal{Q}$ is (ϵ, δ) -differentially private if for all datasets X and X' differ by a unique data record, given any arbitrary event $\mathcal{S} \subseteq \mathcal{Q}$ pertaining to the outcome of the query, the randomized mechanism satisfies the following inequality*

$$Pr(\tilde{q}(X) \in \mathcal{S}) \leq e^\epsilon Pr(\tilde{q}(X') \in \mathcal{S}) + \delta, \quad (1)$$

where $Pr(\mathcal{A})$ denotes the probability of the event \mathcal{A} and the PMF used to calculate the events probability is $f(\tilde{q}|X)$.

Conventionally, given the random published answer \tilde{q} in the differential privacy literature, the *privacy loss* function name is a synonym for the log-likelihood ratio:

$$L_{xx'}(\tilde{q}) \triangleq \ln \frac{f_{\tilde{q}}(\tilde{q}|X)}{f_{\tilde{q}}(\tilde{q}|X')}, \quad (2)$$

where $X \in \mathcal{X}$ is the set of data used to compute the query and X' is an alternative set with a unique attribute or data point that is different. For each X we denote by $\mathcal{X}_X^{(1)}$ the neighborhood of set of X which contains all data sets $X' \in \mathcal{X}$ that differ from X by a predefined sensitive attribute we want to conceal. Note that, if the event $L_{xx'}(\tilde{q}) < 0$ under the experiment with distribution $f(\tilde{q}|X)$ then, in classical statistics, the observer of the outcomes \tilde{q} will choose erroneously the alternative hypothesis that X' was queried (where the emission probability is $f(\tilde{q}|X')$) rather than X . By looking at the tail of the distribution for $L_{xx'}(\tilde{q}) > 0$ under the distribution $f(\tilde{q}|X)$, one can gain insights into how frequently the mechanism allows to differentiate X from X' with great confidence, leaking private information to the observer.

We now introduce the definition of (ϵ, δ) -probabilistic differential privacy (PDP) we consider in this paper, which applies to any random quantity \tilde{q} for any given X :

Definition 2 ((ϵ, δ) -Probabilistic DP [14]). *Consider random data that can come from a set of emission probabilities $\tilde{q} \sim f(\tilde{q}|X)$ that change depending on $X \in \mathcal{X}$. The data \tilde{q} are (ϵ, δ) -probabilistic differentially private $\forall X \in \mathcal{X}$ and $X' \in \mathcal{X}_X^{(1)}$, iff:*

$$\delta \geq \delta_q^\epsilon \triangleq \sup_{X \in \mathcal{X}} \sup_{X' \in \mathcal{X}_X^{(1)}} Pr(L_{xx'}(\tilde{q}) > \epsilon), \quad (3)$$

and the PMF used to calculate the probability is $f(\tilde{q}|X)$.

The following theorem guarantees that (ϵ, δ) -PDP is a strictly stronger condition than (ϵ, δ) -DP.

Theorem 1 (PDP implies DP [15]). *If a randomized mechanism is (ϵ, δ) -PDP, then it is also (ϵ, δ) -DP, i.e.,*

$$(\epsilon, \delta) - PDP \Rightarrow (\epsilon, \delta) - DP, \text{ but } (\epsilon, \delta) - DP \not\Rightarrow (\epsilon, \delta) - PDP.$$

The proof of Theorem 1 is shown in [15], [16].

In our setup $\mathbb{Q}(X)$ is a scalar value in $\mathcal{Q} \equiv [n]$. The query response \tilde{q} is obtained by adding a discrete noise η , whose distribution is denoted by $f(\eta)$, i.e.:

$$\tilde{q} = \mathbb{Q}(X) + \eta \Rightarrow f_{\tilde{q}}(\tilde{q}|X) = f_\eta(\tilde{q} - \mathbb{Q}(X)). \quad (4)$$

The PMF associated with the privacy loss function, called privacy leakage probability, for the additive noise mechanism can be derived from (2), (3) and (4):

$$Pr(L_{xx'}(\tilde{q}) > \epsilon) = Pr\left(\ln \frac{f_\eta(\tilde{q} - \mathbb{Q}(X))}{f_\eta(\tilde{q} - \mathbb{Q}(X'))} > \epsilon\right). \quad (5)$$

For the discrete query case, we denote the “distance one set” of $X \in \mathcal{X}$ as $\mathcal{X}_X^{(1)} \subset \mathcal{X} \setminus X$ and let:

$$\mu_{xx'} \triangleq \mathbb{Q}(X) - \mathbb{Q}(X'), \quad \forall X \in \mathcal{X}, \forall X' \in \mathcal{X}_X^{(1)}. \quad (6)$$

where X' differs from X for one user data record or a sensitive user attribute. Let us define the indicator function

$u_{xx'}(\eta)$, $\eta \in [n]$ such that i^{th} entry is one if $L_{xx'}(\tilde{q}_i) > \epsilon$ and zero otherwise, i.e.:

$$u_{xx'}(\eta) \triangleq \begin{cases} 1, & f(\eta) > e^\epsilon f(\eta + \mu_{xx'}) \\ 0, & \text{otherwise} \end{cases} \quad (7)$$

where we omitted the suffix η and used $f(\eta)$ in lieu of $f_\eta(\eta)$. It is easy to verify that we have:

$$Pr(L_{xx'}(\tilde{q}) > \epsilon) = \sum_{\eta=0}^n u_{xx'}(\eta) f(\eta).$$

Prior to describing our design framework in Section 3, a few considerations on $(\epsilon, \delta) - PDP$ are in order.

2.1 Post-processing

A randomized DP mechanism maps a query output onto a distribution designed to meet Definition (1) or (3). In [17] it was pointed out that, unless $\delta = 0$, in general $(\epsilon, \delta) - PDP$ with $\delta > 0$ cannot be guaranteed after post-processing. The proposition below provides guarantees for $(\epsilon, \delta) - PDP$.

Proposition 1. *Let $\tilde{q} \in \mathcal{Q}$ be a randomized $(\epsilon, \delta) - PDP$ response for the query $q \in \mathcal{Q}$. Let $g : \mathcal{Q} \rightarrow \mathcal{Q}$ be an arbitrary invertible mapping. Then $g \circ \tilde{q} = g(\tilde{q})$ is also a $(\epsilon, \delta) - PDP$ response for any $\delta \geq 0$. Furthermore, if $\delta = 0$, $\epsilon - PDP$ is preserved, irrespective of g .*

Proof. The proof is in Appendix A. \square

Proposition 1 indirectly clarifies the importance of designing randomized responses whose domain is consistent with the query output, since it does not require post-processing to generate answers in the right domain. In fact, the objections in [17] are valid for mechanisms that include post-processing like clamping after adding unbounded noise, where $(\epsilon, \delta) - DP$ are guaranteed prior to the post-processing step, but not after, unless $\delta = 0$. Clamping is not bijective and changes the masses of probability in a way that alters δ for a given ϵ .

3 OPTIMAL ADDITIVE NOISE

For queries $q = \mathbb{Q}(X) \in [n]$, a possible approach other than clamping is to assume that the noise addition is modulo $n+1$ with $\eta \in [n]$, so that the outcome $\tilde{q} = q + \eta \pmod{n+1}$, is always in the appropriate range. In this paper, we seek to obtain the optimum noise distribution $f(\eta)$ for such a mechanism. Since $(\epsilon, \delta) - PDP$ implies $(\epsilon, \delta) - DP$ and hence, it is a stronger notion, we use the definition of $(\epsilon, \delta) - PDP$ throughout.

Next, we omit the $\pmod{n+1}$ to streamline the notation, with the understanding that, from now on, sums and differences of query outcomes and of noise values are always modulo $n+1$. Observe that adding uniform noise would lead necessarily to a scalar query \tilde{q} being uniform and thus, high privacy (i.e. $\delta = 0$ for any $\epsilon > 0$) but poor accuracy since $1 - 1/(n+1)$. This motivates the search for an optimal solution. Using (5) and (6):

$$Pr(L_{xx'}(\tilde{q}) > \epsilon) = Pr\left(\ln \frac{f(\eta)}{f(\eta + \mu_{xx'})} > \epsilon\right). \quad (8)$$

The reasons for using the modulo addition of noise are:

- The randomized answers fall within the range expected for the query, which allows us to leverage Proposition 1.
- The mechanisms requires defining a single distribution rather than distinct distributions for all possible $X \in \mathcal{X}$.
- In the optimization, any pair with the same modulo difference results in a single $(\epsilon, \delta) - PDP$ constraint, simplifying the search for the optimum distribution.
- The simplifications allow us to derive the optimum distribution in closed form for specific use cases.

From (8) it is evident that the (ϵ, δ) privacy curve is entirely defined by the noise distribution and its change due to a shift in the mean. As a result, the probability mass $f(q + \eta)$ is obtained as a circular shift of the PMF $f(\eta)$; therefore (8) can be used with the denominator $f(\eta + \mu_{xx'})$ also representing a circular shift of $f(\eta)$. This result motivates us to define the neighborhood sets, using only $\mu_{xx'}$, in Section 3.2.

3.1 Numerical Optimization

In this section, we show that the problem of finding an optimal additive noise mechanism for a given pair (ϵ, δ) and expected distortion cost can be cast into a MILP formulation, i.e. an optimization problem with linear cost, linear equality and inequality constraints, and real as well as integer variables. While MILPs are non-convex, there are several stable solvers that have convergence guarantees. Our MILP formulation (in (14a)-(14g)) finds optimum noise distributions minimizing a specified expected distortion cost:

$$\mathbb{E}[\rho(\eta)] = \sum_{\eta=0}^n \rho(\eta) f(\eta). \quad (9)$$

There are two typical metrics:

Definition 3 (Error Rate). For $\tilde{q} = \mathbb{Q}(X) + \eta$, error rate has $\rho(\eta) = 1, \eta > 0, \rho(0) = 0$, i.e.:

$$\rho^{ER} \triangleq 1 - f(0). \quad (10)$$

Definition 4 (Mean Squared Error). For $\tilde{q} = \mathbb{Q}(X) + \eta$, the mean squared error (MSE) corresponds to $\rho(\eta) = \eta^2$:

$$\rho^{MSE} \triangleq \mathbb{E}[|\tilde{q} - \mathbb{Q}(X)|^2] = \sum_{\eta=1}^n \eta^2 f(\eta). \quad (11)$$

Remark 1. In the case of an ‘ordered’ query domain, the MSE metric can be preferable over an error rate metric. That is why we are focusing on the minimization of any linear cost in the MILP formulation. However, the numerical results shown in Section 4 indicate that even when we target the error rate metric $\rho^{ER} = 1 - f(0)$, the optimal solution tends to have values that diminish as they move away from the actual query.

Because our analytical results in Section 3.2 consider the error rate metric, whenever ρ is mentioned without specification, this implies ρ^{ER} is being discussed. Having established the cost, the constraints (see (14b)-(14h)) are derived as follows. From the databases, we calculate the set $\{\mu_{xx'}\}$ using (6), which are the only database parameters needed in the formulation. As we know, the sum of probability masses is 1 (see (14b)). The indicator function $u_{xx'}(\eta)$, defined in (7), can be mapped on the integrality constraint, $u_{xx'}(\eta) \in \{0, 1\}, \forall X \in \mathcal{X}, \forall X' \in \mathcal{X}_X^{(1)}$ (see 14h) and on

two linear inequality constraints, $f(\eta) - e^\epsilon f(\eta + \mu_{xx'}) - u_{xx'}(\eta) \leq 0$ and $e^\epsilon f(\eta + \mu_{xx'}) - f(\eta) + e^\epsilon u_{xx'}(\eta) \leq e^\epsilon$ (see (14f) and (14g)). We can rewrite (8) as $Pr(L_{xx'}(\tilde{q}) > \epsilon) = Pr(f(\eta) > e^\epsilon f(\eta + \mu_{xx'})) = \sum_{\eta=0}^n u_{xx'}(\eta) f(\eta) \leq \delta$, $\forall X \in \mathcal{X}, \forall X' \in \mathcal{X}_X^{(1)}$. Since it is a bilinear constraint, and for a MILP formulation we need the constraints to be linear, we introduce the auxiliary variables $y_\eta, \eta \in [n]$:

$$y_\eta \triangleq u_{xx'}(\eta) f(\eta), \quad \eta \in [n]. \quad (12)$$

so that we can use $\sum_{\eta=0}^n y_\eta \leq \delta$ to constrain δ instead; to enforce $y_\eta = f(\eta)$ for $u_{xx'}(\eta) = 1$, and $y_\eta = 0$ for $u_{xx'}(\eta) = 0$, the trick is to use, respectively, the following linear constraints: $u_{xx'}(\eta) + f(\eta) - y_\eta \leq 1$, $u_{xx'}(\eta) - f(\eta) + y_\eta \leq 1$,¹ and $y_\eta - u_{xx'}(\eta) \leq 0$.² This completes the explanation of the optimization constraints shown in (14c)-(14e).³ Let

$$\mathcal{M} \triangleq \{\mu_{xx'} | \mu_{xx'} = \mathbb{Q}(X) - \mathbb{Q}(X'), \forall X \in \mathcal{X}, \forall X' \in \mathcal{X}_X^{(1)}\} \quad (13)$$

The form of the MILP is:

$$\min_{f(\eta), u_{xx'}(\eta), y_\eta} \sum_{\eta=0}^n \rho(\eta) f(\eta) \quad (14a)$$

$$\sum_{\eta=0}^n f(\eta) = 1, \quad (14b)$$

$$\sum_{\eta=0}^n y_\eta \leq \delta, \quad y_\eta - u_{xx'}(\eta) \leq 0, \quad (14c)$$

$$u_{xx'}(\eta) + f(\eta) - y_\eta \leq 1, \quad (14d)$$

$$u_{xx'}(\eta) - f(\eta) + y_\eta \leq 1, \quad (14e)$$

$$f(\eta) - e^\epsilon f(\eta + \mu_{xx'}) - u_{xx'}(\eta) \leq 0, \quad (14f)$$

$$e^\epsilon f(\eta + \mu_{xx'}) - f(\eta) + e^\epsilon u_{xx'}(\eta) \leq e^\epsilon, \quad (14g)$$

$$f(\eta), y_\eta \in [0, 1], \quad \eta \in [n],$$

$$u_{xx'}(\eta) \in \{0, 1\}, \quad \forall \mu_{xx'} \in \mathcal{M}. \quad (14h)$$

The MILP has $3(n+1)$ variables out of which $f(\eta)$ and y_η , $\eta \in [n]$ are real numbers ($2(n+1)$ in total) in $[0, 1]$ and $u_{xx'}(\eta)$ (also $(n+1)$ in number) are integers $\{0, 1\}$; and when $\delta = 0$, it reduces to the linear program (LP):

$$\min_{f(\eta), u_{xx'}(\eta), y_\eta} \sum_{\eta=0}^n \rho(\eta) f(\eta) \quad (15a)$$

$$\sum_{\eta=0}^n f(\eta) = 1, \quad (15b)$$

$$f(\eta) - e^\epsilon f(\eta + \mu_{xx'}) \leq 0, \quad \eta \in [n], \quad (15c)$$

$$f(\eta) \in [0, 1], \quad \forall \mu_{xx'} \in \mathcal{M} \quad (15d)$$

A possible useful variant of the optimization in (14) that will explore in our numerical results is to minimize δ instead, under a distortion constraint, i.e.:

$$\min_{f(\eta), u_{xx'}(\eta), y_\eta} \delta \quad (16a)$$

$$\sum_{\eta=0}^n \rho(\eta) f(\eta) \leq \bar{\rho}, \quad (16b)$$

1. This inequality ensures that $y_\eta = f(\eta)$ if $u_{xx'}(\eta) = 1$.

2. This inequality ensures that $y_\eta = 0$ when $u_{xx'}(\eta) = 0$.

3. Note that other constraints can be added, for instance, that of having a zero mean distribution, or forcing some of the PMF values to be identical, etc.

$$(14b) - \dots - (14h) \quad (16c)$$

In the next sections, we derive analytical solutions of (14) that minimize the error probability $\rho^{ER} = 1 - f(0)$ for some special database structures and corroborate the results in Section 4 comparing the formulas with the MILP solutions obtained using Gurobi [18] as a solver.

3.2 Analytical Solutions

In this section, we analytically study the solution that minimizes the error rate $\mathbb{E}[\rho(\eta)] = 1 - f(0)$. To give closed-form solutions for the optimum PMF, we focus on the following instances of possible $\mu_{xx'}$:

Definition 5 (Single Distance). In this setting $\forall X \in \mathcal{X}, \forall X' \in \mathcal{X}_X^{(1)}$, the difference $\mu_{xx'}$ is constant, i.e. $\mu_{xx'} = \hat{\mu}$. Note that $\hat{\mu} \leq n$.

Definition 6 (Bounded Difference (BD)). In this setting $\forall X \in \mathcal{X}, \forall X' \in \mathcal{X}_X^{(1)}$ $\mu_{xx'}$ take values in the set $[\bar{\mu}]_+$, $\bar{\mu} \leq n$, at least once.

The most general case is the following:

Definition 7 (Arbitrary). In this case $\mu_{xx'}$ can take values from any subset of $[n]$, $\forall X \in \mathcal{X}, \forall X' \in \mathcal{X}_X^{(1)}$.

The next lemma clarifies that the optimum PMF for the BD case for a given (ϵ, δ) is useful to attain the same guarantees for the case of an arbitrary neighborhood.

Lemma 1. Suppose $\bar{\mu} = \sup_{X \in \mathcal{X}, X' \in \mathcal{X}_X^{(1)}} \mu_{xx'}$. Then any noise PMF that provides (ϵ, δ) privacy for the BD neighborhood with parameter $\bar{\mu}$ will give the same guarantees in terms of (ϵ, δ) and ρ for the case of arbitrary neighborhoods. However, lower distortion is achievable by solving the MILP in (14).

Proof. The proof is simple: the set of constraints that need to be met to satisfy (ϵ, δ) privacy for the arbitrary case is a subset of the BD neighborhood case with $\bar{\mu}$ as a parameter. This also means, however, that the minimum ρ^* for the latter case is sub-optimum. \square

Note that the single distance (SD) neighborhood setting is a simple case while the previous lemma indicates that the BD case is more useful in general.

Next we find an explicit solution for the optimum noise PMF $f^*(\eta), \eta \in [n]$ for the SD and BD neighborhood cases. In Section 3.2.4, we discuss the case of discrete vector queries whose entries are independently subjected to the mechanism vs. the optimal solution.

3.2.1 PMF for Single Distance neighborhood

The natural way to express the optimum PMF for an SD neighborhood setting is by specifying the probability masses sorted in decreasing order of $f(k), \forall k \in [n]$. They are referred to as $\{f_{(k)} | 1 \geq f_{(0)} \geq f_{(1)} \geq \dots \geq f_{(n)} \geq 0\}$.

Lemma 2. Considering the case in Definition 5 where $\mu_{xx'} = \hat{\mu}$ is constant $\forall X \in \mathcal{X}, \forall X' \in \mathcal{X}_X^{(1)}$, the noise PMF minimizing the error rate is such that $f_{(h)}^* = f^*(h\hat{\mu}), \forall h \in [n]$ and the inequality in (15c), can be written in term of the sorted PMF as follows:

$$f_{(h)}^* - e^\epsilon f_{(h+1)}^* \leq 0, \quad \forall h \in [n]. \quad (17)$$

Proof. The proof is in Appendix B. \square

To start, let us consider the case $\delta = 0$:

Lemma 3. For the SD neighborhood and $\delta = 0$, the optimal noise PMF for the modulo addition mechanism is:

Case 1: If $(\hat{\mu}, (n+1))$ are relatively prime.

$$f_{(k)}^* = e^{-k\epsilon} f_{(0)}^*, \quad k \in [n]_+, \quad (18a)$$

$$f_{(0)}^* = \frac{1 - e^{-\epsilon}}{1 - e^{-(n+1)\epsilon}} \equiv f^*(0). \quad (18b)$$

Case 2: If $(\hat{\mu}, (n+1))$ are not relatively prime.

$$f_{(k)}^* = e^{-k\epsilon} f_{(0)}^*, \quad k \in [N_{\hat{\mu}} - 1]_+ \quad (19a)$$

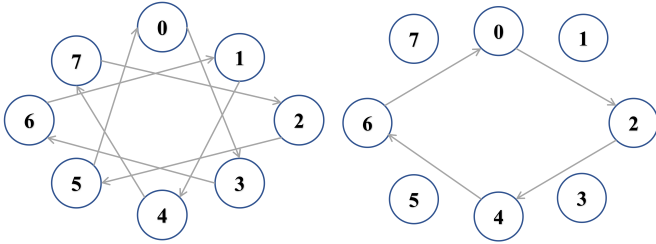
$$f_{(k)}^* = 0, \quad k \in [n] \setminus [i\hat{\mu}], \quad \forall i \in [N_{\hat{\mu}} - 1] \quad (19b)$$

$$f_{(0)}^* = \frac{1 - e^{-\epsilon}}{1 - e^{-(N_{\hat{\mu}})\epsilon}} \equiv f^*(0). \quad (19c)$$

where $N_{\hat{\mu}} = \frac{(n+1)}{\gcd((n+1), \hat{\mu})}$ and $\rho^* = 1 - f^*(0)$.

Proof. The proof is in Appendix C. \square

Lemma 3 is verified numerically in Section 4 in both Case 1 and 2 (see Fig. 9). We illustrate the two cases in Fig. 1.



(a) Case 1: $\hat{\mu} = 3$, $n = 7$, here (3, 8) are relatively prime. (b) Case 2: $\hat{\mu} = 2$, $n = 7$, here (2, 8) are not relatively prime.

Fig. 1: In these examples $f^*(\hat{\mu})$ is single distance, $\hat{\mu}$, away from $f^*(0)$ hence it is assigned $e^{-\epsilon} f^*(0)$, next $f^*(2\hat{\mu})$ is assigned $e^{-2\epsilon} f^*(0)$ since it is $2\hat{\mu}$ away from $f^*(0)$ and so on and so forth. So the order of assignment of values for plot (a) example is: 0, 3, 6, 1, 4, 7, 2, 5 and the order of assignment of values for plot (b) example is: 0, 2, 4, 6. Since the values at 1, 3, 5, 7 are not $\hat{\mu}$ away from $f^*(2k\hat{\mu})$, $k \in [N_{\hat{\mu}} - 1] = 3$ they are assigned 0 value to have a higher $f^*(0)$.

From (18b) we can observe that for case 1, the error rate ρ^* depends only on ϵ and n , and for case 2 (see (19c)), ρ^* depends on both ϵ and $N_{\hat{\mu}}$.

Remark 2. It is notable that in this formulation where the cost is the error rate, positive probability masses corresponding to higher noise outcomes tend to be less likely than those having smaller outcomes. This is why these designs exhibit low MSE.

Mechanisms with better error rate (lower ρ) must allow for $\delta > 0$. It can be proven (see Theorem 2) that the optimal error rate $\rho^*(\delta, \epsilon)$ vs. δ curve is piece-wise linear, interleaving flat regions with intervals with linear negative slope, see Fig. 2. We categorize them as “linear regions” and “flat regions”. Let $\underline{\delta}_k^\epsilon$ and $\bar{\delta}_k^\epsilon$ be the instances of δ at which $\rho^*(\delta, \epsilon)$ changes from k^{th} linear region to k^{th} flat region and k^{th} flat region to $(k+1)^{th}$ linear region, respectively.

Remark 3. We state the following results of this section, i.e., Section 3.2.1, for the case $(n+1, \hat{\mu})$ that are relatively prime. For

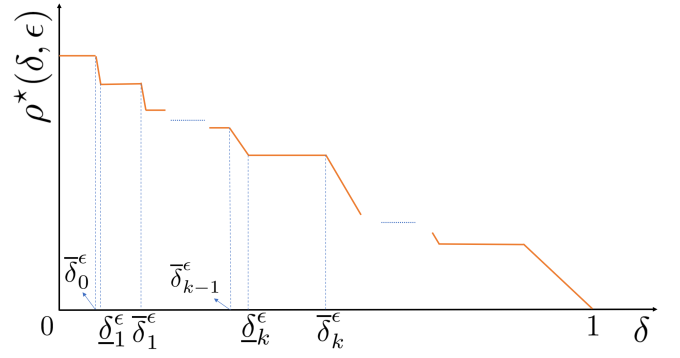


Fig. 2: The variation of ρ as a function of δ for single distance (SD) neighborhood showing the alternate flat and linear regions.

the case where they are not, the results are obtained by replacing n with $N_{\hat{\mu}} = \frac{(n+1)}{\gcd((n+1), \hat{\mu})}$ in all the expressions and explanations.

Let us define the following quantities:

$$\bar{\delta}_k^\epsilon := e^{-(n-k-1)\epsilon} \frac{1 - e^{-\epsilon}}{1 - e^{-(n-k+1)\epsilon}}, \quad \text{for } k \in [n-1] \quad (20a)$$

$$\bar{\delta}_n^\epsilon := 1, \quad \underline{\delta}_0^\epsilon := 0 \quad (20b)$$

$$\underline{\delta}_k^\epsilon := e^{-(n-k)\epsilon} \frac{1 - e^{-\epsilon}}{1 - e^{-(n-k+1)\epsilon}}, \quad \text{for } k \in [n]_+. \quad (20c)$$

Theorem 2. For a given $\epsilon > 0$, the minimum error rate $\rho^*(\delta, \epsilon)$ for $\mu_{XX'} = \hat{\mu}$, $\forall X \in \mathcal{X}, \forall X' \in \mathcal{X}_X^{(1)}$ (i.e. the SD neighborhood) is a piece-wise linear function with respect to $\delta \in [0, 1]$ and the entries of optimum PMF sorted in decreasing order, similarly, alternates k different trends depending on the values of δ . Specifically, for $k = 0$, the expressions of $f_{(h)}^*$ in Lemma 3 are valid between $0 = \underline{\delta}_0^\epsilon \leq \delta \leq \bar{\delta}_0^\epsilon$. For the remaining $k \in [n]_+$, in the k^{th} section where $\rho^*(\delta, \epsilon)$ is flat within $\underline{\delta}_k^\epsilon \leq \delta \leq \bar{\delta}_k^\epsilon$:

$$f_{(h)}^* = \begin{cases} \underline{\delta}_k^\epsilon e^{(n-k-h)\epsilon}, & h \in [n-k], \\ 0, & h \in [n-k+1 : n], \end{cases} \quad (21)$$

In the portion of the k^{th} section where $\rho^*(\delta, \epsilon)$ decreases linearly with δ , which are within $\bar{\delta}_{k-1}^\epsilon < \delta \leq \underline{\delta}_k^\epsilon$:

$$f_{(h)}^* = \begin{cases} \delta e^{(n-k-h)\epsilon}, & h \in [n-k], \\ e^{(n-h)\epsilon} \frac{e^\epsilon - 1}{e^{k\epsilon} - 1} \left(1 - \frac{\delta}{\underline{\delta}_k^\epsilon}\right), & h \in [n-k+1 : n]. \end{cases} \quad (22)$$

and $\rho^*(\delta, \epsilon) = 1 - f_{(0)}^*$.

Proof. The proof is in Appendix D. \square

From Theorem 2 we note that the boundary point $\bar{\delta}_k^\epsilon$ determines the value of $f_{(n-k)}^*$, which is the smallest non-zero probability mass in the k^{th} flat region. Similarly, the other boundary point $\underline{\delta}_k^\epsilon \equiv e^\epsilon \bar{\delta}_k^\epsilon$ indicates the value of $f_{(n-k-1)}^*$, which is the smallest non-zero probability mass in the $(k-1)^{th}$ flat region. Having calculated the optimal PMF for the SD neighborhood case in Theorem 2, the (ϵ, δ) curves correspond to $f^*(0) = 1 - \rho^*$ for all its $n+1$ possible expressions or, better stated, they are the level curves $\rho(\delta, \epsilon) = \rho^*$. The trend of δ curves is monotonically

decreasing with respect to ϵ for a given ρ^* . Let $\epsilon_0^{\rho^*}$ be the solution obtained setting $f^*(0)$ in (18b) to be equal to $1 - \rho^*$:

$$\epsilon_0^{\rho^*} : \rho^* = 1 - \frac{1 - e^{-\epsilon_0^{\rho^*}}}{1 - e^{-(n+1)\epsilon_0^{\rho^*}}} \quad (23)$$

Then we must have that $\delta = 0$ for $\epsilon \geq \epsilon_0^{\rho^*}$. Because this corresponds to a flat region for $f^*(0)$, there has to be a discontinuity moving towards lower values $\epsilon < \epsilon_0^{\rho^*}$, and δ must immediately jump to $\bar{\delta}_0^{\epsilon_0^{\rho^*}}$ when ϵ is an infinitesimal amount below $\epsilon_0^{\rho^*}$. This point is the edge of the *linear region*. For a range of values of $\epsilon < \epsilon_0^{\rho^*}$, δ with respect to ϵ must have the negative exponential trend $\delta = (1 - \rho^*)e^{-n\epsilon}$ obtained from equation (22) for $h = 0, k = 1$ until the next jump occurs, for a value $\epsilon_1^{\rho^*}$ which is obtained by setting $f^*(0)$ for $h = 0$ and $k = 1$ in (21) to be equal to $1 - \rho^*$:

$$\epsilon_1^{\rho^*} : \rho^* = 1 - \bar{\delta}_1^{\epsilon_1^{\rho^*}} e^{(n-1)\epsilon_1^{\rho^*}} = 1 - \frac{1 - e^{-\epsilon_1^{\rho^*}}}{1 - e^{-n\epsilon_1^{\rho^*}}}. \quad (24)$$

Following this logic, one can prove that the optimum (ϵ, δ) curve for a given error rate ρ^* is:

Corollary 1. For a given $\epsilon > 0$, the privacy loss for the SD neighborhood case with the optimal noise mechanism, is a discontinuous function of ϵ , where:

$$\delta^\epsilon = e^{-(n-k)\epsilon}(1 - \rho^*), \quad \epsilon_k^{\rho^*} \leq \epsilon < \epsilon_{k-1}^{\rho^*} \quad (25)$$

when $\rho^* = 1 - f^*(0)$ is in k^{th} section, $k \in [n]_+$ and $\epsilon_k^{\rho^*}$ are the solutions of the following equations:

$$\epsilon_k^{\rho^*} : \rho^* = 1 - \bar{\delta}_k^{\epsilon_k^{\rho^*}} e^{(n-k)\epsilon_k^{\rho^*}} = 1 - \frac{1 - e^{-\epsilon_k^{\rho^*}}}{1 - e^{-(n+1-k)\epsilon_k^{\rho^*}}}. \quad (26)$$

Proof. As discussed before the Corollary, for $\delta = 0$, the level curves of $\rho^*(\delta, \epsilon) = \rho^*$ as a function of ϵ must be monotonically decreasing for $\epsilon \geq \epsilon_0^{\rho^*}$ (see (23)) as ϵ increases. Then the curve will have discontinuities that correspond to the flat regions and the trend between these discontinuities is obtained through the equation $(1 - \rho^*) = f^*(0) = \delta e^{(n-k)\epsilon}$, which implies $\delta = (1 - \rho^*)e^{-(n-k)\epsilon}$. The k^{th} interval starts at the point $\epsilon = \epsilon_k^{\rho^*}$ such that $\delta = \bar{\delta}_k^{\epsilon_k^{\rho^*}}$ ensures that $f^*(0) = 1 - \rho^*$; thus, $\epsilon = \epsilon_k^{\rho^*}$ must be the solution of (26). \square

3.2.2 The Bounded Difference (BD) neighborhood

Also in this case we first start with the optimum noise for $\delta = 0$. First, let us express n as:

$$n = b\bar{\mu} + r \quad (27)$$

where $b = \lfloor n/\bar{\mu} \rfloor$ and $r \in [\bar{\mu} - 1]$. For this case, the inequalities in (15c) can be written as the following:

$$f^*(h) - e^\epsilon f^*(h + \mu) \leq 0, \quad \forall h \in [n], \forall \mu \in [\bar{\mu}]_+. \quad (28)$$

Lemma 4. In the case of a BD neighborhood of size $\bar{\mu}$, the optimum PMF $f^*(\eta)$ has the following form for $i \in [b+1]_+$:

$$f^*(\eta) = f^*(0)e^{-i\epsilon} \equiv \phi_i, \quad (i-1)\bar{\mu} + 1 \leq \eta \leq \min(i\bar{\mu}, n). \quad (29)$$

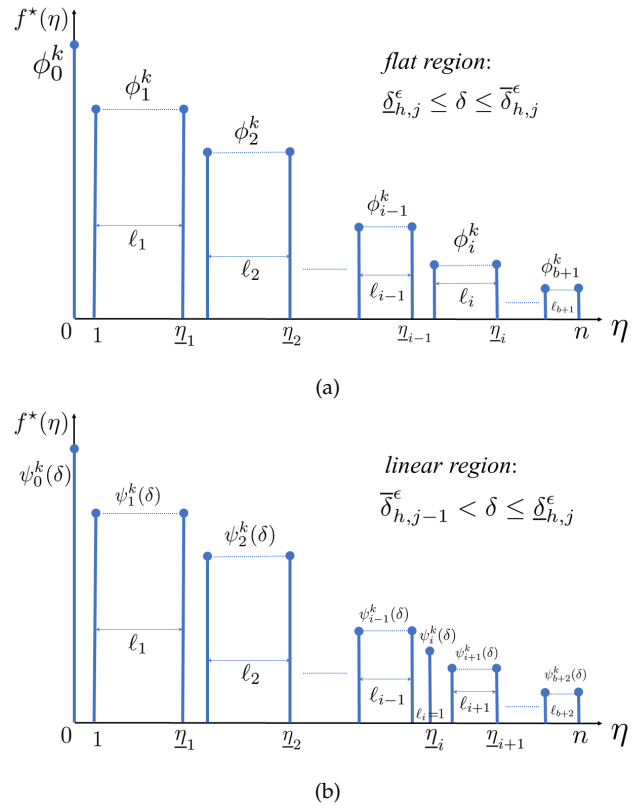


Fig. 3: The PMF of the optimal noise mechanism for the BD neighborhood follows a staircase pattern. In the flat region, it has $b + 1$ steps and i^{th} step height is ϕ_i^k . Similarly, in the linear region, the PMF has $b + 2$ steps and i^{th} step height is $\psi_i^k(\delta)$.

and the mass at zero is:

$$f^*(0) = \left(1 + \bar{\mu} \sum_{i=1}^b e^{-i\epsilon} + r e^{-(b+1)\epsilon} \right)^{-1} \equiv \phi_0. \quad (30)$$

The PMF has, therefore, a staircase trend with steps of length $\ell_i = \bar{\mu}$ for $i \in [b]_+$ and $\ell_{b+1} = r$ and $\rho^* = 1 - \phi_0$.

Proof. The proof is similar to that of Lemma 3 because it recognizes that it is best to meet the inequalities in (28) as equalities, since that allows for the largest $f^*(0)$. The only difference is that the masses in the first group $[\bar{\mu}]_+$ are equal to $\phi_1 = e^{-\epsilon} f^*(0)$, thus they constrain a second group to have value $\phi_2 = e^{-\epsilon} \phi_1$ and so on. There are b of them that contain $\bar{\mu}$ masses of probability and only the last group includes the last r values. $f^*(0)$ is obtained normalizing the PMF to add up to 1. \square

The PMF for $\delta > 0$ has staircase pattern (see Fig. 3), similar to Lemma 4 and, also in this case, for $\delta > 0$ the $\rho^*(\delta, \epsilon)$ has a piece-wise linear trend that alternates between flat and linear regions. However, the BD neighborhood case has an intricate pattern in which the constraints become violations, as the privacy loss $\delta \rightarrow 1$. Rather than having $k = n$, the number of sections k is quadratic with respect to b . To explain the trend, it is best to divide the section of the $f^*(0) \equiv 1 - \rho^*(\delta, \epsilon)$ curve vs. δ in b segments, indexed by $h \in [b]_+$ as shown in Fig. 4. Except for the last interval corresponding to $h = b$, the other segments, indexed by $h \in [b-1]_+$, are further divided into h segments, indexed

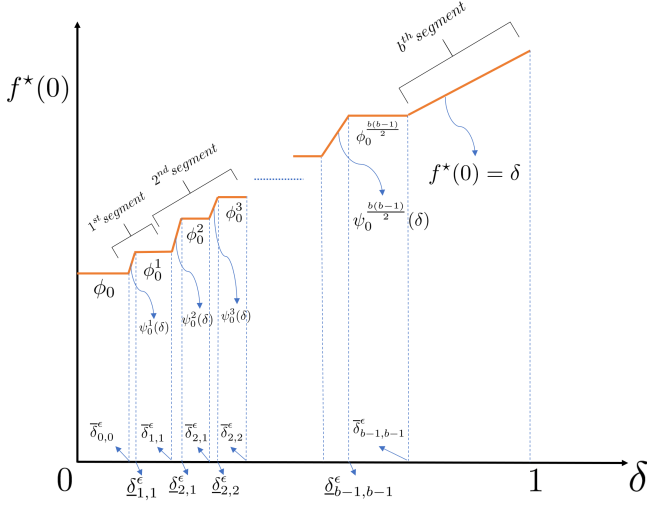


Fig. 4: The variation of $f^*(0)$ as a function of δ for bounded difference (BD) neighborhood showing b segments with the alternate flat and linear regions.

by $j \in [h]_+$ and this index refers to one of the alternating flat and linear regions within the h^{th} interval. This results in $k = \frac{b(b-1)}{2}$ alternating flat and linear regions. Instead, in the segment indexed by $h = b$, there is only one linear region i.e., $f^*(0) = \delta$. The optimum distribution is specified in the following theorem:

Theorem 3. Let $b + r < \bar{\mu}$. For a given $\epsilon > 0$ and for $\mu_{xx'} \in [\bar{\mu}]_+$, $\forall X \in \mathcal{X}, \forall X' \in \mathcal{X}_X^{(1)}$ (i.e. the BD neighborhood), $f^*(0)$ versus δ features flat and linear regions as shown in Fig. 4. In the first $(b-1)$ segments, indexed by $h \in [b-1]_+$, each alternating a pair of flat and linear regions indexed $j \in [h]_+$, with respective boundaries $\delta_{h,j}^\epsilon \leq \delta \leq \bar{\delta}_{h,j}^\epsilon$ and $\bar{\delta}_{h,j-1}^\epsilon < \delta \leq \delta_{h,j}^\epsilon$, with the convention $\bar{\delta}_{h,0}^\epsilon = \bar{\delta}_{h-1,h-1}^\epsilon$. The following facts are true:

(a) In the k^{th} flat region, $k = \sum_{j'=1}^{h-1} j' + j = \frac{(h-1)h}{2} + j$, the optimum PMF (c.f. Fig. 3a) for $i \in [b+1]_+$ is:

$$f^*(\eta) = f^*(0)e^{-i\epsilon} \equiv \phi_i^k, \quad \eta_{i-1} < \eta \leq \eta_i, \quad \eta_0 = 0, \quad (31)$$

where what distinguishes the distributions for each k are the intervals $\eta_{i-1} < \eta \leq \eta_i$, $i \in [b+1]_+$ with equal probability mass ϕ_i^k . More specifically, considering the k^{th} flat region, corresponding to the pair h, j with $h \in [b-1]_+$, $j \in [h]_+$, the intervals $\eta_{i-1} < \eta \leq \eta_i$ of the optimum PMF, for $i \in [b+1]_+$, have lengths $\ell_i = \eta_i - \eta_{i-1}$:

$$\ell_i = \begin{cases} 1, & \text{for } i = 0 \\ \bar{\mu}, & \text{for } i \in [b-h]_+ \\ \bar{\mu} - 1, & \text{for } i \in [b-h+1:b], i \neq b-h+j+1 \\ \bar{\mu}, & \text{for } i = b-h+j+1 \text{ when } j \neq h \\ r + h - u_{hj}, & \text{for } i = b+1. \end{cases} \quad (32)$$

$$u_{hj} := \begin{cases} 1, & \text{for } j \neq h, \\ 0, & \text{for } j = h. \end{cases} \quad (33)$$

The corresponding indexes sets are obtained as:

$$\eta_0 = 0, \quad \eta_i = \eta_{i-1} + \ell_i, \quad i \in [b+1]_+. \quad (34)$$

To normalize the distribution $f^*(0) = \phi_0^k$ must be:

$$\phi_0^k = \frac{1}{\sum_{i=0}^{b+1} \ell_i e^{-i\epsilon}} = (\bar{\mu} \alpha_{hj}^\epsilon + \beta_{hj}^\epsilon)^{-1}, \quad (35)$$

$$\alpha_{hj}^\epsilon := e^{-\epsilon} \xi_b^\epsilon - (1 - u_{hj}) e^{-(b-h+j+1)\epsilon}, \quad \xi_a^\epsilon := \sum_{i'=0}^{a-1} e^{-i'\epsilon}, \quad \forall a \in \mathbb{N}^+ \quad (36)$$

$$\beta_{hj}^\epsilon := 1 + e^{-(b-h+1)\epsilon} (e^{-j\epsilon} - \xi_h^\epsilon) + (r + h - u_{hj}) e^{-(b+1)\epsilon} \quad (37)$$

and the PMF is valid within $\underline{\delta}_{h,j}^\epsilon \leq \delta \leq \bar{\delta}_{h,j}^\epsilon$ where:

$$\bar{\delta}_{h,j}^\epsilon = \phi_0^k e^{-(b-h)\epsilon} \sum_{j'=0}^j e^{-j'\epsilon} = \phi_0^k e^{-(b-h)\epsilon} \xi_{j+1}^\epsilon, \quad j \in [h-1] \quad (38a)$$

$$\bar{\delta}_{h,h}^\epsilon = \phi_0^k e^{-(b-h-1)\epsilon}, \quad \bar{\delta}_{0,0}^\epsilon = \phi_0 e^{-(b-1)\epsilon}, \quad (38a)$$

$$\underline{\delta}_{h,j}^\epsilon = \phi_0^k e^{-(b-h)\epsilon} \xi_j^\epsilon \equiv \left(\frac{\phi_0^k}{\phi_{0,j-1}^k} \right) \bar{\delta}_{h,j-1}^\epsilon \quad (38b)$$

(b) In each of the linear regions, i.e., $\bar{\delta}_{h,j-1}^\epsilon < \delta \leq \underline{\delta}_{h,j}^\epsilon$, the PMF values vary linearly in groups with respect to δ . The group lengths are:

$$\ell_i = \begin{cases} 1, & \text{for } i = 0 \\ \bar{\mu}, & \text{for } i \in [b-h]_+ \\ \bar{\mu} - 1, & \text{for } i \in [b-h+1:b], i \neq b-h+j+1 \\ 1, & \text{for } i = b-h+j+1 \\ r + h - 1, & \text{for } i = b+2 \end{cases} \quad (39)$$

each with probability $\psi_i^k(\delta)$ (as shown in Fig. 3b):

$$\psi_i^k(\delta) = \begin{cases} \delta e^{(b-h-i)\epsilon} / \xi_j^\epsilon, & i \in [b-h+j] \\ \delta e^{(b-h-i+1)\epsilon} / \xi_j^\epsilon, & i \in [b-h+j+2:b+2], \end{cases} \quad (40)$$

$$\psi_i^{b-h+j+1}(\delta) = 1 - \sum_{i=0}^{b+2} \ell_i \psi_i^k(\delta).$$

(c) In the b^{th} segment, i.e. $\bar{\delta}_{b-1,b-1}^\epsilon < \delta \leq 1$, the objective function maximum $f^*(0) = \delta$. So any set of $f^*(\eta)$, $\eta \in [n]$, that satisfy $\sum_{\eta=1}^n f^*(\eta) = 1 - \delta$ and $u_{xx'}(0) = 1, u_{xx'}(\eta) = 0, \eta \in [n]_+$, provides the optimal PMF. One of the possible solutions is:

$$f^*(0) = \delta, \quad (41)$$

$$f^*(\eta) = \frac{1 - \delta}{n}, \quad \eta \in [n]_+. \quad (42)$$

Note that, in the last segment, the optimal PMF no longer follows the staircase pattern.

Proof. The proof is in Appendix E. \square

In Theorem 3 we cover the case $b+r < \bar{\mu}$. When $b+r \geq \bar{\mu}$ the result is not conceptually difficult, but the optimal PMF is hard to express in a readable form. We discuss the general case towards the end of Appendix E.

Corollary 2. For a given $\epsilon > 0$, the privacy loss for the BD neighborhood case with the optimal noise mechanism is also a discontinuous function of ϵ , where:

$$\delta^\epsilon = \xi_j^\epsilon e^{-(b-h)\epsilon} (1 - \rho^*), \quad \epsilon_{h,j}^{\rho^*} \leq \epsilon < \epsilon_{h,j-1}^{\rho^*} \quad (43)$$

when $\rho^* = 1 - \psi_0^k(\delta)$ is in k^{th} section, $k \in \left[\frac{b(b-1)}{2}\right]_+$ and $\epsilon_{h,j}^{\rho^*}$, $h \in [b-1]_+$, $j \in [h]_+$, are the solutions of:

$$\epsilon_{h,j}^{\rho^*} : \rho^* = 1 - \phi_0^k = 1 - \left(\bar{\mu} \alpha_b^{\epsilon_{h,j}^{\rho^*}} + \beta_{h,j}^{\epsilon_{h,j}^{\rho^*}} \right)^{-1}. \quad (44)$$

Proof. The proof is a direct extension of that for Corollary 1 and is omitted for brevity. \square

3.2.3 Optimal Error Rates as $n \rightarrow \infty$

In this section, we study the limit for $n \rightarrow \infty$ of the distributions for the two cases we studied, the SD and BD neighborhoods. First, we discuss the $\delta = 0$ case. The goal is to find the relationship between ϵ and ρ when $n \rightarrow \infty$. From Lemma 3 (18b), we see that for SD neighborhood case, $f^*(0) \equiv 1 - \rho^*(\epsilon) \rightarrow 1 - e^{-\epsilon} \implies \rho^*(\epsilon) \rightarrow e^{-\epsilon}$ as $n \rightarrow \infty$. Since, $\rho^*(\epsilon)$ is also constrained by 0.5, we have that the limit function $\rho_\infty^*(\epsilon)$:

$$\rho_\infty^*(\epsilon) = \begin{cases} 0.5, & \epsilon \in (0, \ln 2] \\ e^{-\epsilon}, & \epsilon \geq \ln 2. \end{cases} \quad (45)$$

And the optimum PMF is zero for all $\eta \neq h\bar{\mu}$, and:

$$f_\infty^*(h\bar{\mu}) = (1 - \rho_\infty^*(\epsilon))e^{-h\epsilon}, \quad h \in \mathbb{N} \quad (46)$$

Similarly, for the BD neighborhood case and $\delta = 0$ in Lemma 4 as $n \rightarrow \infty \implies b \rightarrow \infty$, from (30) we get:

$$\phi_0 \equiv 1 - \rho^*(\epsilon) \rightarrow \left(1 + \frac{\bar{\mu}e^{-\epsilon}}{1 - e^{-\epsilon}} \right)^{-1} \quad (47)$$

$$\implies \rho^*(\epsilon) \rightarrow \frac{\bar{\mu}e^{-\epsilon}}{\bar{\mu}e^{-\epsilon} + (1 - e^{-\epsilon})} \quad (48)$$

Hence, the expression for $\rho^*(\epsilon)$ for any $\epsilon > 0$ is:

$$\rho_\infty^*(\epsilon) = \begin{cases} 0.5, & \epsilon \in (0, \ln(1 + \bar{\mu})] \\ \frac{\bar{\mu}e^{-\epsilon}}{\bar{\mu}e^{-\epsilon} + (1 - e^{-\epsilon})}, & \epsilon \geq \ln(1 + \bar{\mu}). \end{cases} \quad (49)$$

Each of the PMF staircase steps becomes of size $\bar{\mu}$ and the values have an exponentially decaying trend:

$$f_\infty^*(0) = 1 - \rho_\infty^*(\epsilon) \quad (50)$$

$$f_\infty^*(\eta) = f_\infty^*(0)e^{-h\epsilon}, \quad (h-1)\bar{\mu} < \eta \leq h\bar{\mu}, \quad h \in \mathbb{N}^+. \quad (51)$$

For $0 < \delta \leq 1$, it is convenient to use the index $i = n - k$ looking at the trend of the distortion from $\delta = 1$, where $f^*(0) = 1$ backward. Because the discontinuities between flat and linear regions happen at the points where $\delta = \delta_{n-i}^\epsilon$, $i \in [n-1]$ we can see from Theorem 2 the distortion for $i \in [n-1]$:

$$f_i^*(0) \leq \frac{1 - e^{-\epsilon}}{1 - e^{-(i+1)\epsilon}} \implies \rho^*(\delta, \epsilon) \geq 1 - \frac{1 - e^{-\epsilon}}{1 - e^{-(i+1)\epsilon}}, \quad (52)$$

and the size of the intervals shrinks like an $o(e^{-i\epsilon})$, as $i \rightarrow +\infty$ quickly leading to the same result as $\delta \rightarrow 0$, where the distortion tends to $e^{-\epsilon}$ as stated before.

Similarly, for the BD neighborhood case, to find the expressions for ϕ_0^∞ and ϕ_i^∞ , it is convenient to use a new index $c = b - h$, looking at the trends of the distortion from $\delta = 1$, where $f^*(0) = 1$, going backwards towards $\delta = 0$. In the b^{th} segment (part (c) of Theorem 3, $f_b^*(\eta) \rightarrow 0$ as $b \rightarrow \infty$ and $n \rightarrow \infty$ for $\eta \in [n]_+$ and thus $f_b^*(0) \rightarrow 1$. For

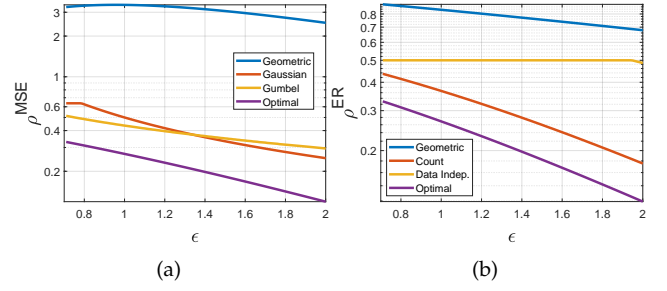


Fig. 5: Comparison of the proposed optimal mechanism in terms of the expected distortion costs with those proposed in [8], [10], [11], [19], [20]. In plot (a), the optimal noise mechanism is compared in terms of mean square error, ρ^{MSE} , with the discrete geometric mechanism, discrete Gaussian mechanism, and Gumbel mechanism for a fixed a value of $\delta = 0.3$ and $n = 8$. In plot (b), the optimal noise mechanism is compared in terms of error rate, ρ^{ER} , with the discrete geometric mechanism, discrete count mechanism, and data independent mechanism for a fixed a value of $\delta = 0.5$ and $n = 7$.

$\delta \approx 1$, in the c^{th} region we get the following expressions by using (35):

$$\alpha_{b-c,j}^\epsilon \rightarrow \frac{e^{-\epsilon}}{1 - e^{-\epsilon}}; \quad \beta_{b-c,j}^\epsilon \rightarrow 1 - \frac{e^{-(c+j+1)\epsilon}}{1 - e^{-\epsilon}} \quad (53)$$

$$\implies \phi_0^\infty(c, j) \rightarrow \frac{1 - e^{-\epsilon}}{\bar{\mu}e^{-\epsilon} + (1 - e^{-\epsilon}(1 + e^{-(c+j)\epsilon}))}, \quad (54)$$

$$\phi_i^\infty \rightarrow e^{-i\epsilon} \phi_0^\infty, \quad i \in [b+1]_+. \quad (55)$$

Now, as $c \rightarrow \infty$, the expression of $\phi_0^\infty(c, j)$ in (54) converges to ϕ_0 as shown in (47), i.e. the result for $\delta \rightarrow 0$.

3.2.4 Optimal Noise Mechanism for Vector Queries

Next, we briefly discuss the optimal noise mechanism design for vector queries to explore what difference it makes to optimize after mapping each vector onto a number in $[n]$ vs. adopting the mechanism on an entry-by-entry basis. In fact, let each entry of a vector query be in the set \mathcal{Q} . In the first case, the MILP formulation of the problem defined in (14a)–(14g) can be applied directly to vectors of queries considering the masses of probabilities as a joint PMF, with arguments corresponding to all possible tuples in \mathcal{Q}^k . In Section 4, we provide two examples for 2D vector queries— one for the BD neighborhood and another for an arbitrary neighborhood (see Fig. 13). We observe that for the BD neighborhood case, the optimum noise mechanism follows a staircase pattern in 2D as well and for the arbitrary neighborhood, the optimum noise mechanism has $e^{-\epsilon} f^*(\mathbf{0})$ values at $\boldsymbol{\eta} = \boldsymbol{\mu}_{xx'}$, where boldface letters are vectors.

Remark 4. In general, the optimal multidimensional noise mechanism does not amount to adding independent random noise to each query entry. In Section 4 we corroborate this statement by showing a counter-example obtained using the MILP program for the vector case, considering a two-dimensional vector query.

4 NUMERICAL RESULTS

First, we compare the performance of our proposed optimal noise mechanism with the discrete geometric mechanism [8], discrete Gaussian mechanism [11], classical exponential mechanism [19], discrete count mechanism [10],

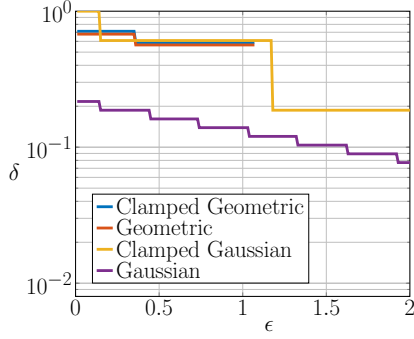


Fig. 6: This plot shows the adverse effect of clamping operation on the (ϵ, δ) trade-off for discrete geometric and discrete Gaussian mechanisms. The following parameters are used: $n = 8, \alpha = 0.7$ and $\sigma^2 = 3.38$.

and data independent mechanism [20]. In plot 5a, the performance is compared in terms of ρ^{MSE} vs. ϵ for a fixed value of $\delta = 0.3$. Similarly, in plot 5b, the performance is compared in terms of ρ^{ER} vs. ϵ for a fixed value of $\delta = 0.5$. From the plots, it is clear that the proposed optimal noise mechanism significantly outperforms all these mechanisms.

Popular mechanisms for discrete queries are adding a random variable from a geometric distribution [8], [21] or a quantized Gaussian distribution (see e.g. [11]). Clamping is an operation in which the query response \tilde{q} is projected onto the domain $[n]$ for any $\eta \in \mathbb{Z}$ [8], i.e.:

$$\tilde{q} = \min(\max(0, q + \eta), n). \quad (56)$$

Let $F_\eta(\eta)$ denote the cumulative distribution function of η ; then the distribution of \tilde{q} in terms of the distribution of η after clamping is as follows:

$$f_{\tilde{q}}(k|q) = \begin{cases} F_\eta(-q), & k = 0 \\ f_\eta(k - q), & k \in [n - 1]_+ \\ 1 - F_\eta(n - q) & k = n. \end{cases} \quad (57)$$

From (57) one can compute the (ϵ, δ) privacy curve using (2), (3) and (57). After clamping the (ϵ, δ) guarantees provided by the said DP mechanisms are different from the ones calculated for $n = +\infty$ as shown in Fig. 6, reported for the same MSE = 3.38. From the figure, it is clear that clamping increases δ for the same ϵ budget, and this effect is particularly pronounced in the case of the Gaussian mechanism. Hence, it is not advisable to use the infinite support-based noise mechanisms, such as discrete geometric and discrete Gaussian, in tandem with clamping operations to publish the discrete query response with finite support.

Next, we now test the modified MILP problem (16a) of minimizing δ , constraining the error rate $\rho = \rho^{ER}$ and solve the MILP numerically using Gurobi as the solver. For a fair comparison, we consider the measure of errors vs. the error rate (ER) and mean square error (MSE), and respective parameters of the noise mechanisms viz., α in [8], σ^2 in [11], β' in [22]⁴, and ρ in [10], [20]; the results are shown in Fig. 7. In plot 7a, we show the comparison of the proposed

4. To realize the classical exponential mechanism based DP [19], we utilize the addition of $Gumbel(\epsilon, \beta')$ distribution to the query inputs [22], where β' is a parameter.

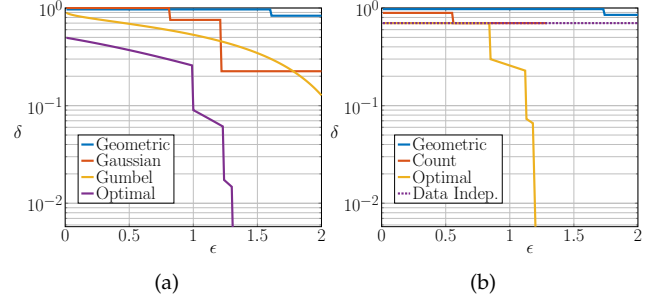


Fig. 7: Comparison of the proposed optimal mechanism in terms of (ϵ, δ) trade-offs with those proposed in [8], [10], [11], [19]. In plot (a), the optimal noise mechanism is compared with the discrete geometric mechanism, discrete Gaussian mechanism and Gumbel mechanism for a fixed MSE, i.e., $\rho_{Gau.}^{MSE} = \rho_{Gum.}^{MSE} = \rho_{Opt.}^{MSE} = 0.6101$ and $n = 8$. In plot (b), the optimal noise mechanism is compared with the discrete geometric mechanism, discrete count mechanism, and data independent mechanism, i.e. $f(0) = 1 - \rho_{Ind.}^{ER}$, $f(\eta) = \rho_{Ind.}^{ER}/n$, $\eta \in [n]_+$, for a fixed ER, i.e., $\rho_{Geo.}^{ER} = \rho_{Cnt.}^{ER} = \rho_{Opt.}^{ER} = \rho_{Ind.}^{ER} = 0.3$ and $n = 7$.

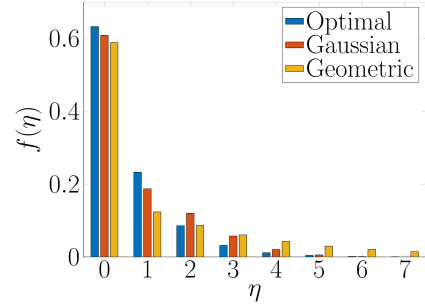


Fig. 8: This plot shows the PMF of the optimal noise mechanism compared with both the Gaussian and geometric mechanisms. The following parameter values are used: $n = 8, \alpha = 0.7, \epsilon = 1$, and $\sigma^2 = 3.38$.

optimal noise mechanism with the discrete geometric, discrete Gaussian, and Gumbel mechanisms for a given MSE = 0.6101. Similarly, in plot 7b, we show the comparison of the proposed optimal noise mechanism with the discrete Gaussian mechanism, discrete count mechanism, and data independent mechanisms for a given ER = 0.3. From the plots, it is clear that the proposed optimal noise mechanism significantly outperforms all these mechanisms $\forall \epsilon > 0$.

Now, we provide the comparison between the PMFs of

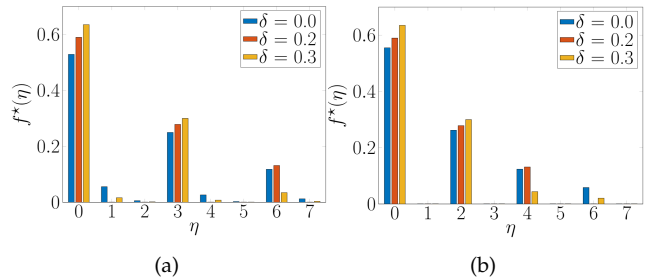


Fig. 9: These plots show the PMF of the optimal noise mechanisms for the SD neighborhood case and the following parameter values are used for both $n = 7, \epsilon = 0.75$. $\hat{\mu} = 3$ is used in plot (a), whereas $\hat{\mu} = 2$ is used in plot (b).

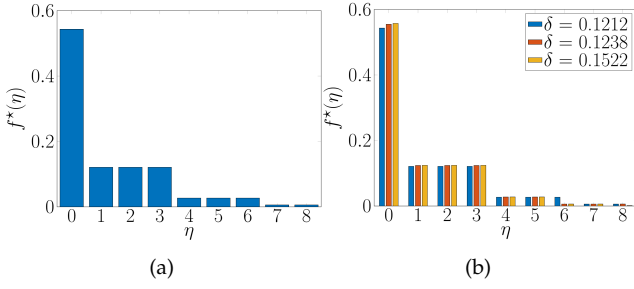


Fig. 10: These plots show the PMF of the optimal noise mechanisms for BD neighborhood case and the following parameter values are used: $n = 8, \bar{\mu} = 3, \epsilon = 1.5$. In plot (a) we see that the optimal noise mechanism follows staircase pattern starting from $\eta = 1$ with $b = 2$ steps of length $\bar{\mu} = 3$ and one last step of length $r = 2$. In plot (b) we show how staircase pattern and step lengths change with δ . It can be seen at $\delta = \delta_0^\epsilon = 0.1212$, $\delta = \delta_1^\epsilon = 0.1238$, and $\delta = \delta_2^\epsilon = 0.1522$ step lengths are: $(1, 3, 3, 2)$ (blue coloured bars), $(1, 3, 2, 3)$ (red coloured bars), and $(1, 3, 2, 2, 1)$ (yellow coloured bars), respectively.

optimal noise distribution with regard to Gaussian and geometric distributions in Fig. 8 for the same MSE parameter for all the distributions. From the plot, we can observe that the probability mass at $\eta = 0$ is maximum for the proposed mechanism, which validates our claim of the least error rate among these mechanisms.

In the following figures, we show the structure of the PMF associated with the optimal noise mechanism. First, we consider the single distance (SD) neighborhood case. More specifically, the plots in Fig. 9 show the PMF of the optimal noise mechanisms, $f^*(\eta), \eta \in [n]$, for SD neighborhood case for $\hat{\mu} = 3$ in Fig. 9a and for $\hat{\mu} = 2$ in Fig. 9b. In the left plot, we see that $f^*(\eta)$ is non-zero for all $\eta \in [n]$ since $(n+1, \hat{\mu})$ are relatively prime but in the right plot, we see that $f^*(\eta)$ is zero for $\eta \in \{1, 3, 5, 7\}$, since $(n+1, \hat{\mu})$ are not relatively prime (see Fig. 1 for the reasoning). From the plots we observe that as δ increases, $f^*(0)$ increases and since error rate, ρ^{ER} , is $1 - f^*(0)$ it decreases with increase in δ . And in the right plot, at some of the $\eta \in [n]_+$ values, zero probability mass is assigned. Hence, we see a higher value of $f^*(0)$ compared to the corresponding values in the left plot, thus having a lower error rate in the right plot for a given δ value. Recall Lemma 2 and Lemma 3, to see that $f^*(0) \geq f^*(3) \geq f^*(6) \geq f^*(1) \geq f^*(4) \geq f^*(7) \geq f^*(2) \geq f^*(5)$ in Fig. 9a which are represented using $f_{(i)}^*, i \in [n]$, respectively. Similarly, we observe $f^*(0) \geq f^*(2) \geq f^*(4) \geq f^*(6)$ and rest $f^*(1) = f^*(3) = f^*(5) = f^*(7) = 0$ in Fig. 9b. Next, we consider the bounded difference (BD) neighborhood case. The plots in Fig. 10 show the PMF of the optimal noise mechanisms, $f^*(\eta), \eta \in [n]$, for BD neighborhood case for $\delta = 0$ in Fig. 10a and for $\delta > 0$ in Fig. 10b. In the left plot, we clearly see the staircase pattern with step sizes equal to $\bar{\mu}$, except for the last step. In the right plot, we see that step widths change as δ increases its values while the staircase structure is maintained. Note that the vertical height of each step is e^ϵ times higher than the previous one, as can be seen in Fig. 10 and in Table 1. Also, from the plot in Fig. 10b and Table 1, one can observe as the value of $f^*(0)$ increases (thus the value of ρ^{ER} decreases) as δ increases, as it is expected.

Next, we consider the vector query case and pro-

TABLE 1: The PMF of the optimal noise mechanism for different values of δ for $n = 8, \bar{\mu} = 3, \epsilon = 1.5$.

	$\delta = 0$	$\delta = 0.1212$	$\delta = 0.1238$	$\delta = 0.1522$
$f^*(0)$	0.5432	0.5432	0.5548	0.5575
$f^*(1)$	0.1212	0.1212	0.1238	0.1244
$f^*(2)$	0.1212	0.1212	0.1238	0.1244
$f^*(3)$	0.1212	0.1212	0.1238	0.1244
$f^*(4)$	0.0270	0.0270	0.0276	0.0278
$f^*(5)$	0.0270	0.0270	0.0276	0.0278
$f^*(6)$	0.0270	0.0270	0.0062	0.0062
$f^*(7)$	0.0060	0.0060	0.0062	0.0062
$f^*(8)$	0.0060	0.0060	0.0062	0.0014

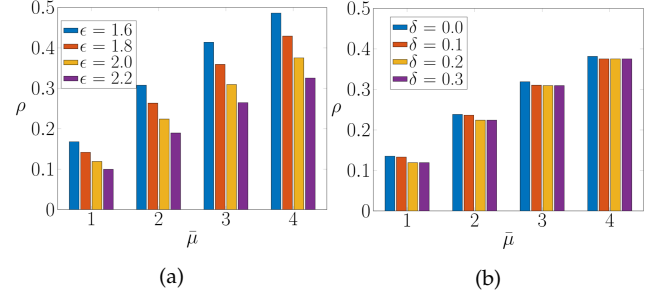


Fig. 11: These plots show the error rate for the BD neighborhood case v/s parameter $\bar{\mu}$. In plot (a) $n = 9, \delta = 0.2$, and in plot (b) $n = 9, \epsilon = 2$ are used.

vide a counter example to support Remark 4 for a two-dimensional vector query. Let $n = 4, \epsilon_1 = 1.5, \epsilon_2 = 1.5, \epsilon = 3, \mu_{X'} = \{0, 1, 2\}, \delta = 0$. The optimal noise mechanism for $(\epsilon_1, 0)$ and $(\epsilon_2, 0)$ DP are: $f_1^*(\eta) = f_2^*(\eta) = [0.6469, 0.1443, 0.1443, 0.0322, 0.0322]$; the values of the optimal noise mechanism PMF $f^*(\eta_1, \eta_2)$ for $(\epsilon, 0)$ are in (58):

$$\begin{bmatrix} 0.6954 & 0.0346 & 0.0346 & 0.0017 & 0.0017 \\ 0.0346 & 0.0346 & 0.0346 & 0.0017 & 0.0017 \\ 0.0346 & 0.0346 & 0.0346 & 0.0017 & 0.0017 \\ 0.0017 & 0.0017 & 0.0017 & 0.0017 & 0.0017 \\ 0.0017 & 0.0017 & 0.0017 & 0.0017 & 0.0017 \end{bmatrix} \quad (58)$$

The marginal distributions happen to be equal, which makes sense in terms of symmetry: $f_1(\eta_1) = \sum_{\eta_2=0}^n f^*(\eta_1, \eta_2) \equiv f_2(\eta_2)$ and they have masses $[0.7681, 0.1073, 0.1073, 0.0086, 0.0086]$. We can observe that $f^*(\eta_1, \eta_2) \neq f_1(\eta_1)f_2(\eta_2)$.

The plots in Figs. 11–14 are self explanatory.

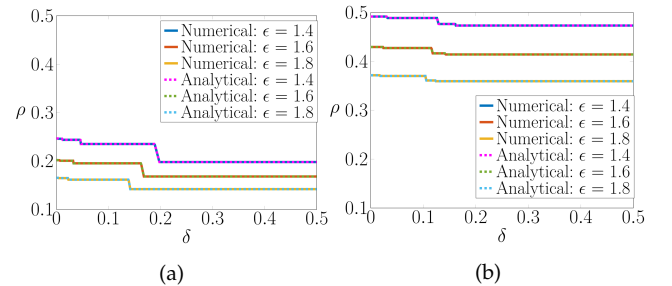


Fig. 12: Error rate ρ for the SD and BD neighborhood cases v/s parameter δ , respectively, confirming the trends predicted by Theorems 2 and 3. In plot (a) $n = 9, \hat{\mu} = 3$ and in plot (b) $n = 9, \bar{\mu} = 3$ are used.

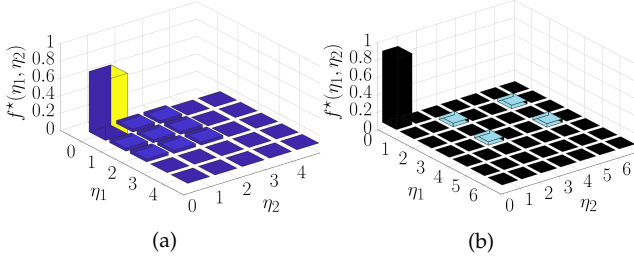


Fig. 13: The optimal noise joint PMF for two-dimensional vector query case for a BD and arbitrary neighborhoods, respectively. In plot (a) the parameters are: $n = 4$, $\epsilon = 3$, $\bar{\mu}_1 = \bar{\mu}_2 = 2$. In this BD neighborhood example, the staircase pattern is similar to the scalar query case in Theorem 3. In plot (b) the following parameters are used: $n = 6$, $\epsilon = 3$, $\mu_1 = \{1, 3\}$, $\mu_2 = \{2, 5\}$. In this arbitrary neighborhood example, the second largest peaks can be observed at the union of distance one set of each dimension, i.e., $[1, 2]$, $[1, 5]$, $[3, 2]$, $[3, 5]$.

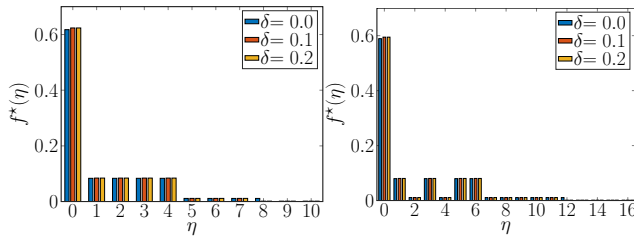


Fig. 14: These plots show the PMF of the optimal noise mechanisms when the Advanced Metering Infrastructure (AMI) database is queried from 1416 houses that belong to 12 distribution circuits across California, USA. We use $\bar{\mu} = \bigcup_{X \in \mathcal{X}} \bigcup_{X' \in \mathcal{X}_X^{(1)}} \mu_{XX'}$. In the left plot, 11 quantization levels are used, hence $n = 10$. In this example, $\bar{\mu} = \{1, 2, 3, 4\}$ is observed. In the right plot, 17 quantization levels are used, hence $n = 16$. In this example, $\bar{\mu} = \{1, 3, 5, 6\}$ is observed. From these figures we observe that $f^*(\eta)$ is considerably larger for $\eta \in \{\bar{\mu} \cup 0\}$ than those $\eta \in [n] \setminus \{\bar{\mu} \cup 0\}$.

5 CONCLUSIONS AND FUTURE WORK

Considering queries whose domain is discrete and finite, in this paper we proposed a novel MILP formulation to determine what is the PMF for an additive noise mechanism that minimizes the error rate of the DP answer for any (ϵ, δ) pair. The modulo addition between the noise and the queried data is modulo $n + 1$ equal to the size of the query domain. For two special cases, which we referred to as the single distance (SD) neighborhood and bounded difference (BD) neighborhood, we have provided closed-form solutions for the optimal noise PMF and its probability of error versus δ for a given ϵ and studied the asymptotic case for $n \rightarrow \infty$. We also compared the proposed optimal noise mechanism to state-of-the-art noise mechanisms and found that it significantly outperforms them for a given error rate or mean square error. In the future, we plan to leverage these results in several applications that have to do with labeling data as well as a building block to study theoretically queries with finite uncountable support as well as the case of vector queries, whose optimum PMF can be calculated with our MILP and does not appear to be the product of the optimum PMFs for each entry.

REFERENCES

- [1] U. Census, "Decennial census: Processing the count: Disclosure avoidance modernization," 2020. [Online]. Available: <https://www.census.gov/programs-surveys/decennial-census/decade/2020/planning-management/process/disclosure-avoidance.html>
- [2] A. Eland. (2015) Tackling urban mobility with technology. Google Policy Europe Blog. [Online]. Available: <https://europe.googleblog.com/2015/11/tackling-urban-mobility-with-technology.html>
- [3] B. Ding, J. Kulkarni, and S. Yekhanin, "Collecting telemetry data privately," *Advances in Neural Information Processing Systems*, vol. 30, pp. 3574–3583, 2017.
- [4] R. Rogers, S. Subramaniam, S. Peng, D. Durfee, S. Lee, S. K. Kanchara, S. Sahay, and P. Ahammad, "Linkedin's audience engagements api: A privacy preserving data analytics system at scale," arXiv:2002.05839, 2020.
- [5] Q. Geng and P. Viswanath, "The optimal noise-adding mechanism in differential privacy," *IEEE Transactions on Information Theory*, vol. 62, no. 2, pp. 925–951, 2015.
- [6] J. Soria-Comas and J. Domingo-Ferrer, "Optimal data-independent noise for differential privacy," *Information Sciences*, vol. 250, pp. 200–214, 2013.
- [7] Q. Geng and P. Viswanath, "Optimal noise adding mechanisms for approximate differential privacy," *IEEE Transactions on Information Theory*, vol. 62, no. 2, pp. 952–969, 2015.
- [8] A. Ghosh, T. Roughgarden, and M. Sundararajan, "Universally utility-maximizing privacy mechanisms," in *Proceedings of the Forty-First Annual ACM Symposium on Theory of Computing*, ser. STOC '09. New York, NY, USA: Association for Computing Machinery, 2009, p. 351–360. [Online]. Available: <https://doi.org/10.1145/1536414.1536464>
- [9] G. Cormode, T. Kulkarni, and D. Srivastava, "Constrained private mechanisms for count data," *IEEE Transactions on Knowledge and Data Engineering*, vol. 33, no. 2, pp. 415–430, 2019.
- [10] P. Sadeghi, S. Asodeh, and F. d. P. Calmon, "Differentially private mechanisms for count queries," arXiv:2007.09374, 2020.
- [11] C. L. Canonne, G. Kamath, and T. Steinke, "The discrete gaussian for differential privacy," *Advances in Neural Information Processing Systems*, vol. 33, pp. 15 676–15 688, 2020.
- [12] Q. Geng, P. Kairouz, S. Oh, and P. Viswanath, "The staircase mechanism in differential privacy," *IEEE Journal of Selected Topics in Signal Processing*, vol. 9, no. 7, pp. 1176–1184, 2015.
- [13] C. Dwork, F. McSherry, K. Nissim, and A. Smith, "Calibrating noise to sensitivity in private data analysis," in *Theory of cryptography conference*. Berlin, Heidelberg: Springer, 2006, p. 265–284.
- [14] A. Machanavajjhala, D. Kifer, J. Abowd, J. Gehrke, and L. Vilhuber, "Privacy: Theory meets practice on the map," in *2008 IEEE 24th international conference on data engineering*. Cancun, Mexico: IEEE, 2008, pp. 277–286.
- [15] D. McClure, "Relaxations of differential privacy and risk/utility evaluations of synthetic data and fidelity measures," Ph.D. dissertation, Duke University, 2015.
- [16] A. Triastcyn and B. Faltings, "Bayesian differential privacy for machine learning," in *International Conference on Machine Learning*. Proceedings of Machine Learning Research: PMLR, 2020, pp. 9583–9592.
- [17] S. Meiser, "Approximate and probabilistic differential privacy definitions," Cryptology ePrint Archive, 2018. [Online]. Available: <https://eprint.iacr.org/2018/277>
- [18] G. O. Solver, "Gurobi," 2021. [Online]. Available: <https://www.gurobi.com/>
- [19] F. McSherry and K. Talwar, "Mechanism design via differential privacy," in *48th Annual IEEE Symposium on Foundations of Computer Science (FOCS'07)*. Providence, RI, USA: IEEE, 2007, pp. 94–103.
- [20] N. Ravi, A. Scaglione, S. Kadam, R. Gentz, S. Peisert, B. Lunghino, E. Levijarvi, and A. Shumavon, "Differentially Private K-Means Clustering Applied to Meter Data Analysis and Synthesis," *IEEE Transactions on Smart Grid*, vol. 13, no. 6, pp. 4801–4814, 2022.
- [21] V. Balcer and S. Vadhan, "Differential privacy on finite computers," arXiv:1709.05396, 2019.
- [22] R. Adams. (2013) The gumbel-max trick for discrete distributions. Department of Computer Science, Princeton University. [Online]. Available: <https://lips.cs.princeton.edu/the-gumbel-max-trick-for-discrete-distributions/>

APPENDIX A

PROOF OF PROPOSITION 1

Let us define the domains of q, \tilde{q} , and $g(\tilde{q})$ to be $\mathcal{Q}_1, \mathcal{Q}_2$, and \mathcal{Q}_3 , respectively. The given function is $g : \mathcal{Q}_2 \rightarrow \mathcal{Q}_3$. We can prove that (ϵ, δ) - PDP is preserved in general under post-processing if $g(\tilde{q})$ is bijective. In fact, in this case $\mathcal{Q}_2 = \mathcal{Q}_3$ and the probability mass of $g(\tilde{q})$ in \mathcal{Q}_3 domain, i.e., $f_{g(\tilde{q})}(g(\tilde{q}))$, is equal to the probability mass of the corresponding argument \tilde{q} . So, $\forall X \in \mathcal{X}, \forall X' \in \mathcal{X}_X^{(1)}$, it is trivial to see that:

$$L_{XX'}(g(\tilde{q})) = L_{XX'}(\tilde{q}) \quad (59)$$

and that the probability δ of the leakage event $L_{XX'}(g(\tilde{q})) > \epsilon$ remains the same. If $\delta = 0$ then the ϵ - PDP is always preserved. The case $|\mathcal{Q}_2| \geq |\mathcal{Q}_3|$ is the interesting one (e.g. clamping): in this case multiple values of $\tilde{q} \in \mathcal{V}_g$ map onto a single value $g(\tilde{q}) = g$. Next, we show that $L_{XX'}(\tilde{q}) \leq \epsilon$ with probability one implies $L_{XX'}(g(\tilde{q})) \leq \epsilon$ with probability one. In fact, since for all \tilde{q} , $f(\tilde{q}|X) \leq e^\epsilon f(\tilde{q}|X')$:

$$\begin{aligned} L_{XX'}(g(\tilde{q})) &= \log \frac{f(g|X)}{f(g|X')} = \log \frac{\sum_{\tilde{q} \in \mathcal{V}_g} f(\tilde{q}|X)}{\sum_{\tilde{q} \in \mathcal{V}_g} f(\tilde{q}|X')} \\ &\leq \log \frac{\sum_{\tilde{q} \in \mathcal{V}_g} e^\epsilon f(\tilde{q}|X')}{\sum_{\tilde{q} \in \mathcal{V}_g} f(\tilde{q}|X')} \leq \epsilon \end{aligned} \quad (60)$$

APPENDIX B

PROOF OF LEMMA 2

When the objective is minimizing error rate, it is natural to introduce the inequality constraint $f_{(0)}^* = f^*(0) \geq 0.5 = 1 - \rho^{ER}$. Hence, $f_{(0)}^* = \sup_{k \in [n]} f_{(k)}^*$. Now, substitute $\eta = 0$ and $\mu_{XX'} = \hat{\mu}$ in (15c) we see that $f^*(0) \leq e^\epsilon f^*(\hat{\mu})$. Since we are minimizing the sum of the mass away from zero, we assign $f^*(\hat{\mu})$ to the minimum possible value, which is $f^*(\hat{\mu}) = e^{-\epsilon} f^*(0)$ in this case. Similarly, from (15c) we see that $f^*(k\hat{\mu}) \leq e^\epsilon f^*((k+1)\hat{\mu})$, $k \in [n-1]_+$, and we are minimizing the sum of the mass away from zero, we need to assign $f^*((k+1)\hat{\mu})$ to the minimum possible value, which is $f^*((k+1)\hat{\mu}) = e^{-\epsilon} f^*(k\hat{\mu})$.⁵ Since $\epsilon > 0$, $f^*(k\hat{\mu}) \geq f^*((k+1)\hat{\mu})$, $\forall k \in [n]$. Hence, we can write $f_{(k)}^* = f^*(k\hat{\mu})$, $\forall k \in [n]$.

APPENDIX C

PROOF OF LEMMA 3

Case 1: $(\hat{\mu}, (n+1))$ are relatively prime.

The proof logic is as follows. Since minimizing the error rate is equivalent to have the maximum mass possible at $\eta = 0$, we expect $f^*(0) = \sup_{\eta \in [n]} f^*(\eta)$. The constraint (17), implies $f^*(\hat{\mu}) \geq e^{-\epsilon} f^*(0)$. Also that for any $\eta = k\hat{\mu}$, $k \in [2 : n]$, $f^*(k\hat{\mu}) \geq e^{-\epsilon} f^*((k-1)\hat{\mu}) \geq e^{-k\epsilon} f^*(0)$ and $f^*((n+1)\hat{\mu}) \geq e^{-\epsilon} f^*(n\hat{\mu})$. From all these inequalities and the constraint (15a), we conclude that what would allow having the largest mass of probability at $\eta = 0$ is meeting all constraints as equality, starting from the first. Since $\hat{\mu}$ and

n are prime, the multiples of $\hat{\mu}$ eventually cover the entire range $[n]$ and therefore: $f^*(k\hat{\mu}) = e^{-k\epsilon} f^*(0)$, $k \in [n]$. This result leads to the optimum distribution in Lemma 3. Now, $f^*(0)$ can be computed as follows:

$$f^*(0) + e^{-\epsilon} f^*(0) + \dots + e^{-n\epsilon} f^*(0) = 1 \quad (61a)$$

$$\Rightarrow f^*(0) = \frac{1 - e^{-\epsilon}}{1 - e^{-(n+1)\epsilon}}. \quad (61b)$$

Case 2: $(\hat{\mu}, (n+1))$ are not relatively prime.

The same argument of Case 1 holds for $k \in [N_{\hat{\mu}} - 1]_+$, where $N_{\hat{\mu}} = \frac{(n+1)}{\gcd((n+1), \hat{\mu})}$, i.e., $f^*(k\hat{\mu}) = e^{-k\epsilon} f^*(0)$, $k \in [N_{\hat{\mu}} - 1]_+$. However in this case, since for $k = N_{\hat{\mu}}$, $f^*(N_{\hat{\mu}}\hat{\mu}) = f^*(0)$ and the cycle repeats over the same exact values covered from zero up to $(N_{\hat{\mu}} - 1)$ which does not include all PMF entries. Since we are minimizing the objective function to satisfy all the inequality constraint $f_{(0)}^* = f^*(0) \geq 0.5 = 1 - \rho^{ER}$ and (17) for all k values that are not constraining $f^*(0)$, the best choice is to assign them zero, i.e., $f^*(k) = 0$, $k \in [n] \setminus [i\hat{\mu}]$, $\forall i \in [N_{\hat{\mu}} - 1]$.

APPENDIX D

PROOF OF THEOREM 2

We focus on Case 1, as Case 2 follows from Remark 3. In Lemma 2, we clarified that it is best to deal with ordered values, and in Lemma 3, we specified $f_{(h)}^*$, $h \in [n]$, as a function of $\epsilon > 0$ for $\delta = 0$. The best solution for $\rho(\epsilon, \delta)$ initially does not change until violating an inequality in (17) yields better accuracy. This happens as soon as the second smallest value $f_{(n-1)}^*$ corresponding to $\delta = 0$ is $f_{(n-1)}^* = \delta$, which is the upper-limit $\bar{\delta}_0$ from (20). The reason why it is $f_{(n-1)}^*$ and not $f_{(n)}^*$ matters because surely $f_{(n)}^* < e^\epsilon f^*(0)$ which in the modulo n sum is the value that follows and that we aim at maximizing. At this point, for $\bar{\delta}_0 < \delta \leq \underline{\delta}_1$ the value of $f_{(n-1)}^* = \delta$, all the values for $0 \leq h < n-1$ meet the constraints with equality and thus $f_{(h)}^* = e^{(n-1-h)\epsilon} \delta$, while the last value $f_{(n)}^*$ progressively diminishes until it becomes zero, as shown in equation (22), at the start of the next flat region. This pattern continues until eventually one by one all $n-1$ masses become zero except for $f^*(0) = 1 = \underline{\delta}_n^\epsilon$.

APPENDIX E

PROOF OF THEOREM 3

In Lemma 4, we have the expressions for ϕ_i , $i \in [b+1]_+$ for $\epsilon > 0$ and $\delta = 0$. The best solution for $\rho^*(\delta, \epsilon)$ does not change w.r.t $\delta > 0$ until violating an inequality in (28) to yield better accuracy. The key to the proof is understanding that the first inequality to be violated occurs when considering δ greater or equal not to the smallest PMF value but to the PMF values of the third to the last group in $\delta = 0$ case, i.e., $\phi_{b-1} = \delta$, whose value equals the first boundary point $\bar{\delta}_{0,0}^\epsilon$ (see (38a)). The inequality violated is with respect to the PMF of the second to the last group, which is ϕ_b , which becomes $= \delta$ and $\phi_{b-1} > e^\epsilon \delta$. The reason why the PMF of the last group, i.e. ϕ_{b+1} , does not violate the inequality in (28) is that $\phi_{b+1} < e^\epsilon \phi_0$ (we use ϕ_0 since we are doing modulo summation) is always true for all members of this group, due to the fact that ϕ_0 is the objective function which we are maximizing. Similarly, the

5. Note that for $f^*(n\hat{\mu})$, there is no choice to assign any value since it will be automatically fixed once $f^*(k\hat{\mu})$, $k \in [n-1]$ values are fixed and it is trivial to see that $f^*(n\hat{\mu}) = \min f^*(k\hat{\mu})$, $\forall k \in [n]$.

PMF of the second last group, i.e. ϕ_b , does not violate the inequality in (28) because some members of this group do not violate the inequality $\phi_b < e^\epsilon \phi_0$ for the same reason as stated above. At this point, for $\bar{\delta}_{0,0} < \delta \leq \underline{\delta}_{1,1}$ the value of $\phi_{b-1} = \delta$, the PMF values for $i \in [b-1]$ meet the constraints with equality and thus $\psi_i^1(\delta) = \delta e^{(b-1-i)\epsilon}$, for $i \in [b-1]$. At this point, the group with PMF ϕ_b , whose length is $\ell_b = \bar{\mu}$, splits into two groups, one of length $\ell_b = (\bar{\mu} - 1)$ and the other with a singleton step $\ell_{b+1} = 1$. This split happens to assign more probability mass at $\psi_0^1(\delta)$, which is our objective, while still violating the constraint in (28) between $\delta = \psi_{b-1}^1(\delta)$ and $\psi_{b+1}^1(\delta)$ in order to lower the error further. For $i = b$ and $i = b+2$, the PMF values satisfy the constraints with equality, hence $\psi_b^1(\delta) = \delta e^{-b\epsilon}$ and $\psi_{b+2}^1(\delta) = \delta e^{-(b+1)\epsilon}$ while the unconstrained singleton step PMF $\psi_{b+1}^1(\delta)$ decreases until it joins the next group since it has matched its value, and becomes ϕ_{b+1}^1 , as shown in equation (31), at the start of the next flat region, i.e., for $\underline{\delta}_{1,1} \leq \delta \leq \bar{\delta}_{1,1}$. In this region, the PMF of every group is $e^{-\epsilon}$ times the PMF of previous group similar to Lemma 4; the only change here is the lengths of b^{th} and $(b+1)^{th}$ groups which are now $\ell_b = (\bar{\mu} - 1)$ and $\ell_{b+1} = r + 1$.

Now we provide the reason for splitting only groups of lengths $\bar{\mu}$ using contradiction. Suppose there is a group i of length $\ell < \bar{\mu}$ which splits at the beginning of a linear region $k \in [b]_+$. As we know, for this group to split there must a violation of the inequality in (28) between the PMF values $\phi_{i-1}^{k-1} = \delta$ and ϕ_i^{k-1} . Now, ϕ_i^{k-1} splits into $\psi_i^k(\delta)$ of length $(\ell - 1)$ and $\psi_{i+1}^k(\delta)$ of length 1, which decreases as δ grows. We see that $\psi_{i+1}^k(\delta)$ is $\leq \bar{\mu}$ distance away from at least two members of the $\psi_{i-1}^k(\delta)$ group leading to at least two violations in the inequalities in (28) which makes the actual privacy loss $\geq 2\delta$, in violation of the inequality constraint in (14c), which is a contradiction.

From the discussion in the previous paragraph, for the next linear region, we now search for a group of length $\bar{\mu}$ with the smallest possible PMF, which is found to be $(b-1)^{th}$ group, whose PMF is ϕ_{b-1}^1 . For this group to split and enter into the linear region, we should have $\delta = \phi_{b-2}^1$. As explained in the first paragraph of this proof, the same process follows in this linear region too, i.e., for $\bar{\delta}_{1,1} < \delta \leq \underline{\delta}_{2,1}$. In the next flat region, i.e., for $\underline{\delta}_{2,1} \leq \delta \leq \bar{\delta}_{2,1}$ the step lengths, as compared to previous flat region, which have been altered are $\ell_{b-1} = (\bar{\mu} - 1)$ and $\ell_b = \bar{\mu}$. Now, observe that b^{th} group has length $\bar{\mu}$ and from the discussion in the previous paragraph, this group splits at the end of this flat region, i.e., when $\delta = \phi_{b-2}^2 + \phi_{b-1}^2 = \phi_0^2 e^{-(b-2)\epsilon} (1 + e^{-\epsilon}) \equiv \bar{\delta}_{2,1}$. In this case the inequality in (28) are violated by both ϕ_{b-2}^2 and ϕ_{b-1}^2 , hence the summation and the reasoning for (38a) (this was missing in SD neighborhood case). For the same reason, in the next linear region i.e., for $\bar{\delta}_{2,1} < \delta \leq \underline{\delta}_{2,2}$ the normalizing factor $(1 + e^{-\epsilon}) \equiv \xi_2^\epsilon$ is used while computing the PMF values in (40).

These alternate flat and linear intervals are formed as δ increases and the process continues until all the remaining groups of lengths $\bar{\mu}$ split into groups of lengths $(\bar{\mu} - 1)$. The expression for $\delta_{h,j}$, $h \in [b-1]_+$, $j \in [h]_+$ in (38b) is computed using $f^*(0)$ vs. δ curve (see Fig. 4) in the linear region between ϕ_0^{k-1} and ϕ_0^k , the slope corresponding to

$\psi_0^k(\delta)$ i.e. $e^{(b-h)\epsilon}/\xi_j^\epsilon$ from (40). i.e.,

$$\begin{aligned} \delta_{h,j} &= \bar{\delta}_{h,j-1}^\epsilon + (\phi_0^k - \phi_0^{k-1}) e^{-(b-h)\epsilon} \xi_j^\epsilon \\ &= \phi_0^{k-1} e^{-(b-h)\epsilon} \xi_j^\epsilon + (\phi_0^k - \phi_0^{k-1}) e^{-(b-h)\epsilon} \xi_j^\epsilon \\ &= \phi_0^k e^{-(b-h)\epsilon} \xi_j^\epsilon. \end{aligned} \quad (62)$$

Now, we find the simplified expression for the value of ϕ_0^k from the fact that $\phi_0^k + \sum_{i=1}^{b+1} \ell_i \phi_i^k = 1$ as following:

$$\begin{aligned} \phi_0^k &\left(1 + \bar{\mu} \sum_{i=1}^{b-h} e^{-i\epsilon} + (\bar{\mu} - 1) \sum_{\substack{i=b-h+1 \\ i \neq b-h+j+1}}^b e^{-i\epsilon} \right. \\ &\quad \left. + \bar{\mu} u_{hj} e^{-(b-h+j+1)\epsilon} + (r+h-u_{hj}) e^{-(b+1)\epsilon} \right) = 1 \end{aligned} \quad (63)$$

By further simplifying, we get:

$$\begin{aligned} \phi_0^k &= \left(1 + \bar{\mu} \sum_{i=1}^b e^{-i\epsilon} - \bar{\mu} (1 - u_{hj}) e^{-(b-h+j+1)\epsilon} \right. \\ &\quad \left. + e^{-(b-h+j+1)\epsilon} + (r+h-u_{hj}) e^{-(b+1)\epsilon} - \sum_{i=b-h+1}^b e^{-i\epsilon} \right)^{-1} \\ \phi_0^k &= (\bar{\mu} \alpha_{hj}^\epsilon + \beta_{hj}^\epsilon)^{-1}, \text{ see (35).} \end{aligned}$$

The last group has length $b+r$ which is less than $\bar{\mu}$ in our case. This assumption simplifies the analysis, hence tractable. Even though the pattern is same, the case $b+r \geq \bar{\mu}$ complicates the analysis because, for $j \in [h]_+$ and for every $h \in [b]_+$, instead of increasing h when $j = h$, j must be increased beyond h to accommodate the groups of lengths $\bar{\mu}$ created by the last group whenever its length $r+h$ exceeds $\bar{\mu}$. Hence, we do not discuss the analysis of this case, but we do provide some numerical results in Section 4.